NANO LETTERS

Letter

Surface Plasmon Resonance Scattering and Absorption of anti-EGFR Antibody Conjugated Gold Nanoparticles in Cancer Diagnostics: Applications in Oral Cancer

Ivan H. El-Sayed, Xiaohua Huang, and Mostafa A. El-Sayed

Nano Lett., **2005**, 5 (5), 829-834 • DOI: 10.1021/nl050074e

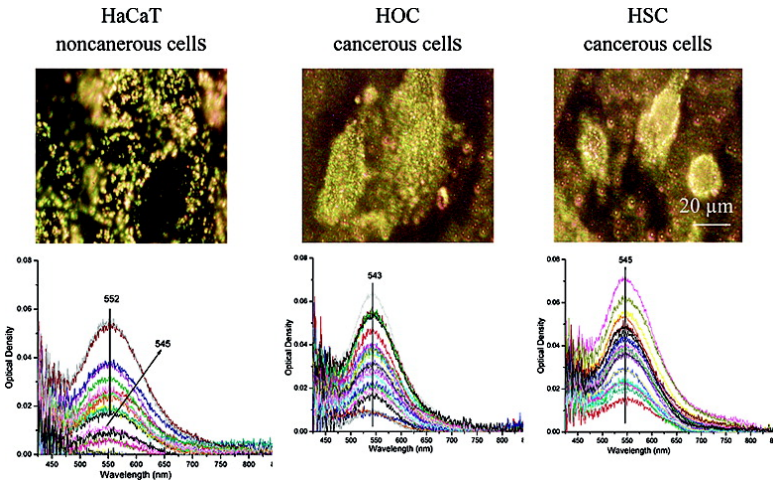

More About This Article

Additional resources and features associated with this article are available within the HTML version:

- Supporting Information
- Links to the 103 articles that cite this article, as of the time of this article download
- Access to high resolution figures
- Links to articles and content related to this article
- Copyright permission to reproduce figures and/or text from this article

View the Full Text HTML

Nano Letters is published by the American Chemical Society. 1155 Sixteenth Street N.W., Washington, DC 20036

NANO LETTERS

2005
Vol. 5, No. 5
829−834

Surface Plasmon Resonance Scattering and Absorption of anti-EGFR Antibody Conjugated Gold Nanoparticles in Cancer Diagnostics: Applications in Oral Cancer

Ivan H. El-Sayed,*,† Xiaohua Huang,‡ and Mostafa A. El-Sayed*,‡

Department of Otolaryngology−Head and Neck Surgery, Comprehensive Cancer Center, University of California at San Francisco, San Francisco, California 94143, and Laser Dynamics Laboratory, School of Chemistry and Biochemistry, Georgia Institute of Technology, Atlanta, Georgia 30332

Received January 13, 2005

ABSTRACT

Gold nanoparticles with unique optical properties may be useful as biosensors in living whole cells. Using a simple and inexpensive technique, we recorded surface plasmon resonance (SPR) scattering images and SPR absorption spectra from both colloidal gold nanoparticles and from gold nanoparticles conjugated to monoclonal anti-epidermal growth factor receptor (anti-EGFR) antibodies after incubation in cell cultures with a nonmalignant epithelial cell line (HaCaT) and two malignant oral epithelial cell lines (HOC 313 clone 8 and HSC 3). Colloidal gold nanoparticles are found in dispersed and aggregated forms within the cell cytoplasm and provide anatomic labeling information, but their uptake is nonspecific for malignant cells. The anti-EGFR antibody conjugated nanoparticles specifically and homogeneously bind to the surface of the cancer type cells with 600% greater affinity than to the noncancerous cells. This specific and homogeneous binding is found to give a relatively sharper SPR absorption band with a red shifted maximum compared to that observed when added to the noncancerous cells. These results suggest that SPR scattering imaging or SPR absorption spectroscopy generated from antibody conjugated gold nanoparticles can be useful in molecular biosensor techniques for the diagnosis and investigation of oral epithelial living cancer cells in vivo and in vitro.

The increasing availability of nanostructures with highly controlled optical properties in the nanometer size range has created widespread interest in their use in biotechnological systems for diagnostic application and biological imaging.[1−2] Cellular imaging utilizing microscope techniques provides anatomic details of cells and tissue architecture important for cancer diagnostics and research. Currently used optical probes include chemiluminescent, fluorimetric, and colorimetric techniques.[3] Markers attached to antibodies provide specific information about the presence of specific molecules. Quantum dots are widely used and studied for this application due to their unique size-dependent fluorescence properties.[4,5] But potential human toxicity and cytotoxicity of the semiconductor material are two major problems for its in vitro and in vivo application. Colloidal gold nanoparticles have become an alternative consideration due to their ease of preparation, ready bioconjugation, and potential noncytotoxicity.[6] Immunogold nanoparticles conjugated to antibodies have provided excellent detection qualities for cellular labeling using electron microscopy.[7]

Gold nanoparticles have the ability to resonantly scatter visible and near-infrared light upon the excitation of their surface plasmon oscillation. The scattering light intensity is extremely sensitive to the size and aggregation state of the particles.[8] Preliminary studies have reported their use as contrast agents for biomedical imaging using confocal scanning optical microscopy,[9] multiphoton plasmon resonance microscopy,[10] optical coherence microscopy,[11] and third-harmonic microscopy.[12] Gold nanoparticles have several advantages for cellular imaging compared to other agents. They scatter light intensely and they are much brighter than chemical fluorophores. They do not photobleach and they can be easily detected in as low as 10^{-16} M concentration.[13] Sokolov[9] described the scattering of anti-EGFR/Au nanoparticles for cervical cancer when stimulated with a laser at single wavelength. Irradiation with a laser will only scatter light that is close to the laser wavelength used. Gold

* Corresponding authors. Ivan El-Sayed: ielsayed@ohns.ucsf.edu. Tel: 415-353-2401, Fax: 415-353-2603; Mostafa El-Sayed: mostafa.el-sayed@chemistry.gatech.edu. Tel: 404-894-0292. Fax: 404-894-0294.
† University of California at San Francisco.
‡ Georgia Institute of Technology.

10.1021/nl050074e CCC: $30.25
Published on Web 04/15/2005

nanoparticles scatter light of many colors when illuminated with white light at appropriate angles. The wavelength distribution of the light in this case is determined by the shape and size of the nanoparticles.[14] This color scattering property offers the potential for labeling studies with a white light source, which has not yet been characterized for cellular imaging and detection.

In the present work, we used a very simple and inexpensive conventional microscope with proper rearrangement of the illumination system and the light collection system to image cells that were incubated with colloidal gold or with anti-epidermal growth factor receptor (anti-EGFR) antibody conjugated gold nanoparticles. The optical properties of the gold nanoparticles incubated in single living cancerous and noncancerous cells are compared for different incubation methods. It is found that the scattering images and the absorption spectra recorded from anti-EGFR antibody conjugated gold nanoparticles incubated with cancerous and noncancerous cells are very different and offer potential techniques for cancer diagnostics.

Gold NPs were prepared by the citrate reduction of chloroauric acid.[15] The nanoparticles have an absorption maximum at 529 nm, and TEM shows that the nanoparticles have an average size of 35 nm. The anti-EGFR/gold conjugates were prepared according to the method described by Sokolov.[8] Briefly, the gold NPs were diluted in 20 mM HEPES buffer (pH 7.4, Sigma) to a final concentration with optical density of 0.8 at 529 nm. 40 uL anti-EGFR monoclonal antibodies (host mouse; Sigma) was added to 960 uL of the same HEPES buffer to form 1 mL dilute solution. Then 10 mL of the gold solution prepared above was mixed with the dilute antibody solution for 20 min. 0.5 mL of 1% poly(ethylene glycol) (MW 20 000; Sigma) was added to the mixture to prevent aggregation, and the solution was centrifuged at 6000 rpm for 30 min. Then the anti-EGFR/gold pellet was redispersed in PBS buffer (pH = 7.4, Cellgro) and stored at 4 °C.

One nonmalignant epithelial cell line HaCaT (human keratinocytes) and two malignant epithelial cell lines HOC 313 clone 8 and HSC 3 (human oral squamous cell carcinoma) were cultured on 18 mm diameter glass cover slips in a 12-well tissue culture plate in DMEM plus 5% FBS at 37 °C under 5% CO_2. The cover slips were coated with collagen type I (Roche) in advance for optimum cell growth. For the incubation of colloidal gold, nanoparticles ($\sim$ 0.3 nM) were added into the medium and the cells were grown for 48 h. The cells on the cover slips were then rinsed with PBS buffer and fixed with 1.6% paraformaldehyde and sealed with another cover slip with a small amount of glycerol. For the incubation of conjugated nanoparticles, the cells were grown on the cover slips for 48 h and then the cell monolayer was immersed into the conjugated nanoparticle solution for 40 min, rinsed with PBS buffer, fixed with paraformaldehyde, and sealed as above.

The light scattering images were taken using an inverted Olympus IX70 microscope in which the illumination system was removed and replaced by an illumination condenser (U-DCW), which delivers a very narrow beam of white light from a mercury lamp on top of the samples. A 100×/1.35 oil Iris Ph3 objective (UPLANAPO) was used to collect only the scattered light from the samples. When the light beam direction is optimized, the center illumination light beam does not enter the light collection cone of the microscope objective, and only the scattered light of the side beam by the sample is collected. This presents an image of a bright object in a dark background. The absorption spectra of gold nanoparticles inside a single cell were measured using a SEE1100 microspectrometer under 20× magnification.

In the present work gold nanoparticles with the average sizes of 35 nm are chosen after experimental determination of the particle uptake efficiency, the cellular labeling efficiency, and the light scattering intensities of the nanoparticles. Gold nanoparticles are introduced into cells by the endocytosis process during cell differentiation and proliferation processes. Smaller nanoparticles cross the cytoplasmic membrane more easily, but their scattering light cross-section is smaller than larger nanoparticles. They also give more greenish scattered color which cannot be easily resolved from the scattered green light from the cellular organelles. Larger nanoparticles have higher scattering cross-section but have smaller labeling efficiency, possibly due to steric hindrance. For this experiment, we also used 15 and 60 nm nanoparticles, but neither one is found to be more efficient than the 35 nm nanoparticles in either the amount of colloid nanoparticles uptaken into cells or the labeling efficiency for cancer cell detection when anti-EGFR antibodies are used.

Figure 1 shows the light scattering images of the HaCaT noncancerous cells (left column), HOC cancerous cells (middle column) and HSC cancerous cells (right column) without nanoparticles. All the cells show dim greenish light (two images were shown for each type of cells for comparison). This green light is due to autofluorescence and scattered light from the cell organelles in cell cytoplasm and membrane. From this figure we can see that the three types of cells have different structure characteristics. HOC cancer cells are almost four times larger than HaCaT or HSC cells. HaCaT and HSC cells show almost homogeneous diamond shapes while HOC cells have other shapes for some cells.

When incubated in the presence of nanoparticles, the cells grow at a normal rate and the nanoparticles are accumulated inside the cells. The incorporated gold nanoparticles scatter strong yellowish light and make individual cells easily identifiable. Three images for each kind of cell are shown to test reproducibility (Figure 2). Examination reveals that gold nanoparticles are predominantly accumulated inside the cytoplasm of the cells. In most HaCaT noncancerous cells (left column) the gold nanoparticles demonstrate a spotted pattern inside the cytoplasm while the nanoparticles are homogeneously distributed in the cytoplasm of HOC (middle column) and HSC (right column) cancerous cells. The difference of the distribution of nanoparticles inside cells may reflect the difference of the cell differentiation and proliferation processes. The HSC specimens give the strongest scattering light due to the large amount of accumulated gold nanoparticles.

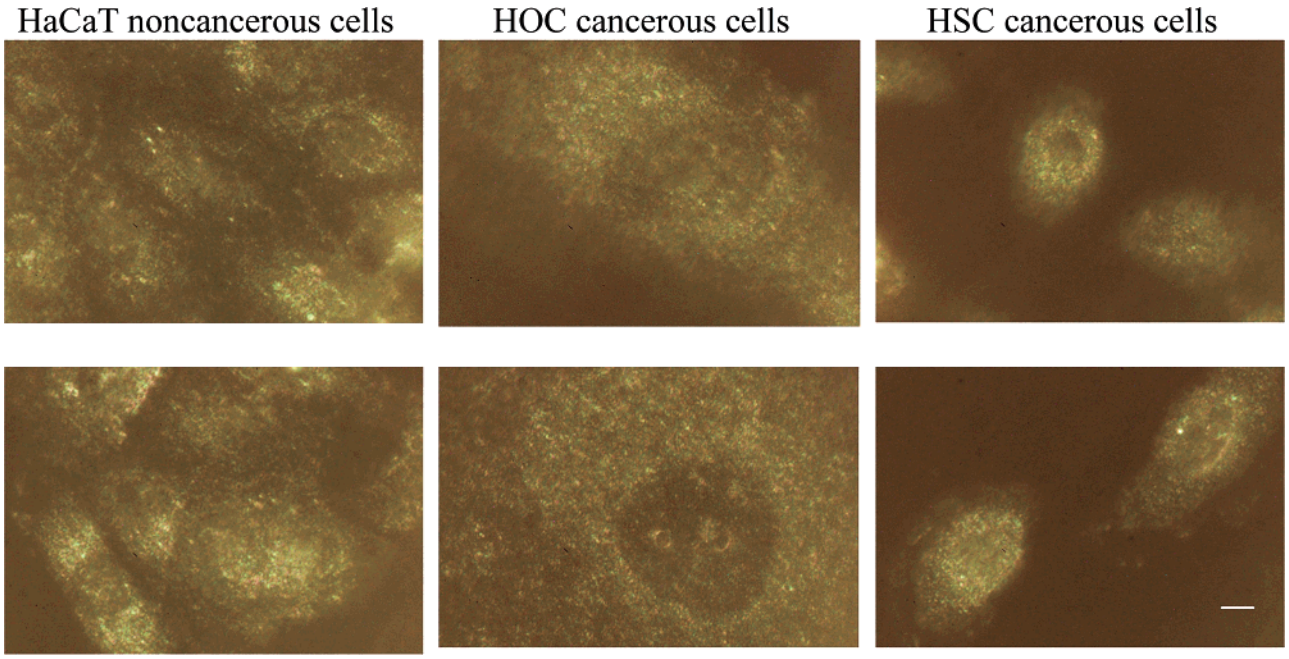

Figure 1. Light scattering images of HaCaT noncancerous cells (left column), HOC cancerous cells (middle column), and HSC cancerous cells (right column) without gold nanoparticles. Two different images of each kind of cells were shown to test reproducibility. The weak greenish scattered light from the cells shows large difference in the sizes and shapes of the three different types of cells. Scale bar: 10 μm for all images.

Using micro-UV−visible spectroscopy, the absorption spectra of gold nanoparticles from single cells are obtained shown in the bottom row of Figure 2. To statistically characterize the surface plasmon absorption of the gold nanoparticles inside the cells, 25 cells of each kind are measured. The NPs inside all cells have a major peak around 545 nm, characteristic of the surface plasmon absorption of the individual nanoparticles inside the cytoplasm of the cells that are red shifted by 16 nm compared to the colloid nanoparticle suspension at 529 nm. This suggests that the nanoparticle surface has a different dielectric environment when present inside the cells. The broad absorption around 700 nm of the gold nanoparticles inside the cells is characteristic of the aggregated gold nanoparticles. Aggregation of the nanoparticles is likely induced by the salts both in the growth medium and in the cytoplasm of the cells. The capping material could also be dissolved inside cells and thus leads to aggregation of the resulting metallic nanostructures. In HSC cells, the aggregates have the absorption maximum around 715 nm. In HaCaT cells, the size of these large aggregates is smaller as concluded from the shorter wavelength surface plasmon absorption maximum. The absorption of the aggregates inside HOC is not as resolved due to the shorter wavelength (679 nm), which is close to the absorption maximum of the surface plasmon absorption of the individual nanoparticles. The different sizes of the aggregates inside different kind of cells may reflect the difference in the cell cytoplasm medium or differences in the intracellular processing of the nanoparticles by the cells. The ability to resolve aggregates within cells by SPRA spectroscopy suggests that different capping agents could be utilized to monitor intracellular processes as aggregates are formed.

The light scattering pattern of gold nanoparticles is significantly different when anti-EGFR antibodies were conjugated to gold nanoparticles before incubation with the cells (Figure 3). The HaCaT noncancerous cells are poorly labeled by the nanoparticles and the cells could not be identified individually (Figure 3, three images on the left column). When the conjugates are incubated with HOC (Figure 3, three images on the middle column) and HSC (Figure 3, three images on the right column) cancerous cells for the same amount of time, the nanoparticles are found on the surface of the cells, especially on the cytoplasm membranes for HSC cancer cells. This contrast difference is due to the specific binding of overexpressed EGFR on the cancer cells with the anti-EGFR antibodies on the gold surface. The nanoparticles are also found on the HaCaT noncancerous cells due to part of the specific binding, but mostly due to the nonspecific interactions between the antibodies and the proteins on the cell surface, and thus the nanoparticles are randomly distributed on the whole cells. The nonspecific interaction between the anti-EGFR antibodies and the collagen matrix also exists, which is shown as the reddish scattering light of the gold nanoparticles on the collagen background.

When anti-EGFR antibodies are attached to the gold nanoparticles, all the absorption spectra on different cells become narrower and similar for each cell type. No absorption bands due to aggregation are observed. The nanoparticles bound to HOC and HSC cancer cells have similar absorption maxima at around 545 nm, which is 9 nm red shifted compared to the isolated anti-EGFR/Au solutions at 536 nm. This red shift is due to the specific binding of the anti-EGFR antibodies on the gold surface to EGFR on the cell surface.

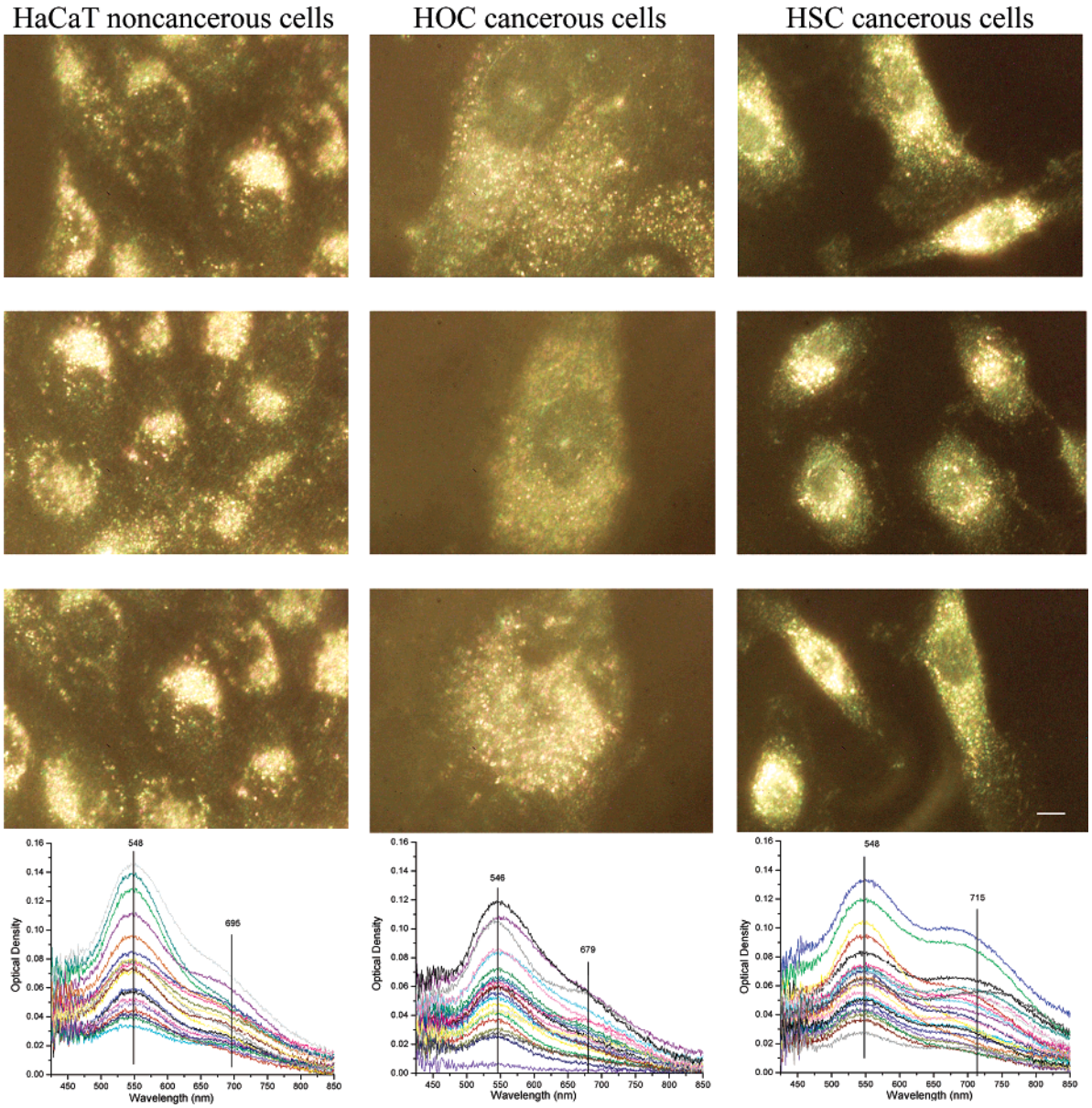

Figure 2. Light scattering images and microabsorption spectra of HaCaT noncancerous cells (left column), HOC cancerous cells (middle column), and HSC cancerous cells (right column) after incubation with unconjugated colloidal gold nanoparticles. Three different images of each kind of cells are shown to test reproducibility. The images show that the particles are inside the cells in the cytoplasm region but do not seem to adsorb strongly on the nuclei of the cells. The absorption spectra were measured for 25 different single cells of each kind. They show that nanoparticles have an SPR absorption maximum around 548 nm, independent of the cell type. The broad long wavelength tails in the absorption spectra suggest the presence of aggregates. It also shows that no specific difference is observed in either the scattering images or the absorption spectra of the gold nanoparticles in the cancerous and the noncancerous cells. Scale bar: 10 μm for all images.

It also could be due to the interparticle interaction resulting from the arrangement of the conjugates on the cell surface in two dimensions. Such spectroscopic binding undoubtedly changes the dielectric constant around the surface of the gold nanoparticles. One can use the maximum at 545 nm to characterize the conjugated nanoparticles binding to the EGFR on the cell surface. For HaCaT noncanerous cells, the particles with maximum at 545 nm are found to have a maximum absorption of 0.01 (Figure 3) for the 25 cells measured. The rest of the nanoparticles have their maximum at 552 nm. This red shift indicates that these nanoparticles are nonspecifically bound. The maximum absorbance of the conjugated particles to cancer cells is of 0.06 for HOC cells and 0.07 for HSC cells. One can conclude that the binding ability of the anti-EGFR antibody conjugated nanoparticles to HOC and HSC cancerous cells is 600% and 700%, respectively, over the HaCaT noncancerous cells. This is undoubtedly due to the difference of the EGFR concentration on the surface of the cancer and noncancerous cells. Current optical staining techniques do not have the ability to quantify nonspecific binding in this manner. Our results correlate well with previously published studies which qualitatively report that most cancerous cells accumulate significantly higher amounts of EGFR during the carcinoma process.[16]

In summary, cellular imaging with improved contrast due to the strong resonant light scattering of gold nanoparticles

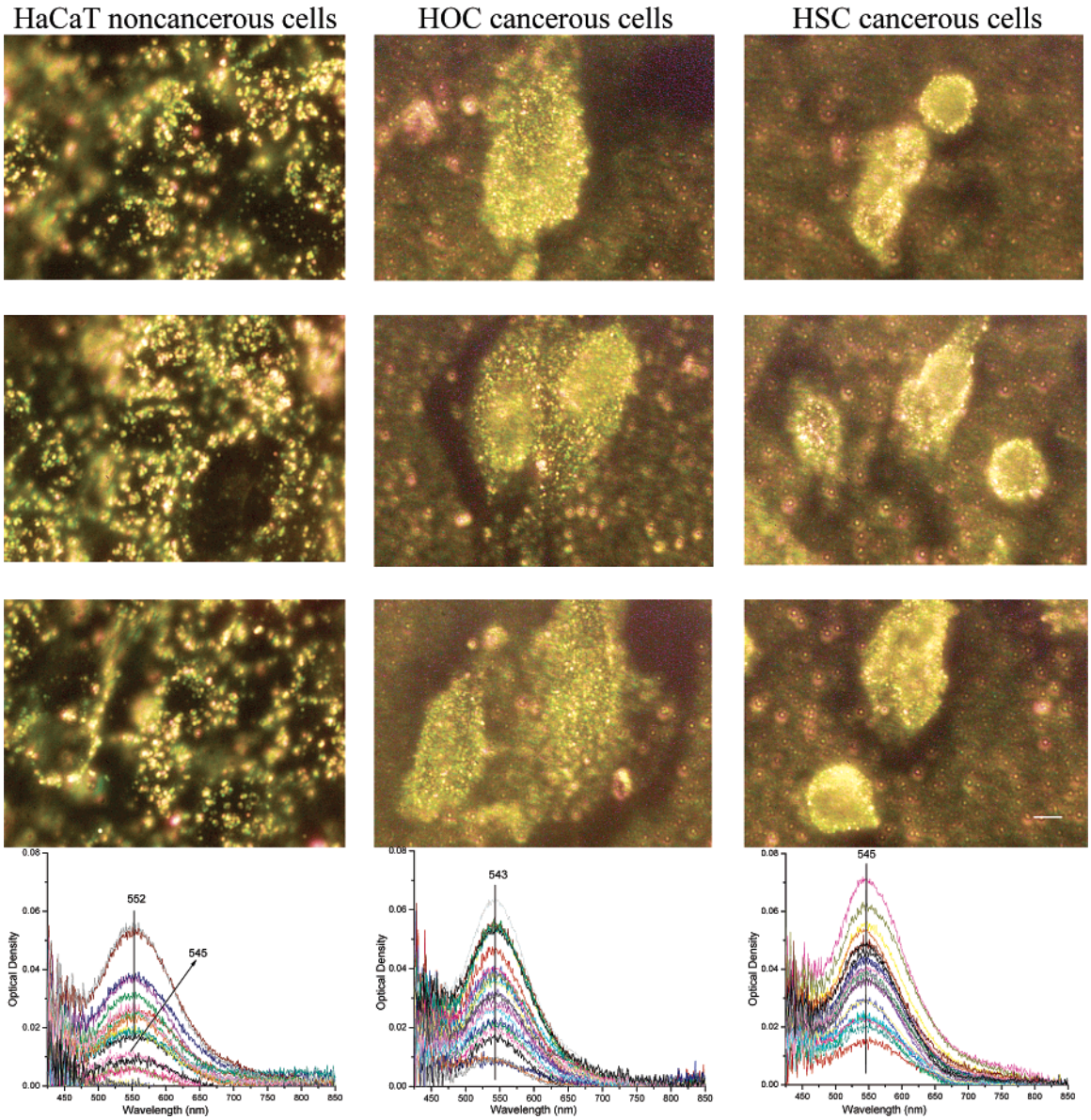

Figure 3. Light scattering images and microabsorption spectra of HaCaT noncancerous cells (left column), HOC cancerous cells (middle column), and HSC cancerous cells (right column) after incubation with anti-EGFR antibody conjugated gold nanoparticles. Three different images of each kind of cells are shown to test reproducibility. The absorption spectra were measured for 25 different single cells. The figure shows clearly distinguished difference for the scattering images from the noncancerous cells (left column) and the cancerous cells (right two columns). The conjugated nanoparticles bind specifically with high concentrations to the surface of the cancer cells (right two columns). Conjugated nanoparticles did not show aggregation tendency (no long wavelength broad tail is observed). Scale bar: 10 μm for all images.

incubated inside or on the surface of cells is obtained using a very simple and inexpensive student microscope with proper rearrangement of the illumination system and the light collection system. The nonconjugated gold nanoparticles are accumulated inside cells and aggregation takes place (Figure 2). The observed difference in the scattering of different types of cells in this figure is mostly due to the difference in the size of the cells (Figure 1) and not to the specific interaction of the nanoparticles with different cells. However, there is a distinct difference in the distribution of anti-epidermal growth factor receptor antibody conjugated nanoparticles when incubated with cancerous and noncancerous cells (Figure 3). Conjugated nanoparticles bind homogeneously and specifically to the surface of the cancer cells (two right columns in Figure 3) with an absorption maximum at 545 nm. The binding to noncancerous cells seems to be nonspecific and at random, with absorption maximum mostly around 552 nm. Thus both SPR scattering imaging and SPR absorption spectroscopy from anti-EGFR antibodies conjugated gold nanoparticles are found to distinguish between cancerous and noncancerous cells. This makes either technique potentially useful in cancer diagnostics.

Acknowledgment. We thank Prof. Paul Edmonds, Prof. Mohan Srinivasarao, Prof. Rob Dickson, Dr. Lynn Peyser, Mr. Sandeep Patel, and Mr. Jie Zheng at the Georgia Institute of Technology for assistance and use of their facilities. I.H.E. thanks Prof. Randall Kramer and Mr. Moon Lim at the Oral

Cancer Research Center at the University of California at San Francisco for their aid, instruction, and use of their facilities, and Dr. Patrica Leake and Dr. Russell Snyder in the Epstein Laboratory (UCSF) for the use of their facilitites. The financial support of the Chemical Science, Geosciences and Bioscience Division of the Department of Energy (NO: DE-FG02-97 ER14799) is acknowledged.

References

(1) Alivisatos, A. P. *Nat. Biotech.* **2004**, *22*, 47−52.
(2) Wickline, S. A.; Lanza, G. M. *Circulation* **2003**, *107*, 1092−1095.
(3) Roda, A.; Pazzagli, M.; Kricka, L. J.; Stanley, P. E. *Bioluminescence and Chemiluminescence: Perspectives for the 21st Century*; Wiley: Chichester, 1999.
(4) Bruchez, M., Jr.; Moronne, M.; Gin, P.; Weiss, S.; Alivisatos, A. P. *Science* **1998**, *281*, 2013−2015.
(5) Chan, W. C. W.; Nie, S. *Science* **1998**, *281*, 2016−2018.
(6) West, J. L.; Halas, N. J. *Cur. Opin. Biotech.* **2002**, *11*, 215−217.
(7) Hayat, M. A. *Colloidal gold: principles, methods and applications*; Academic Press: San Diego, 1989; Vol 1.
(8) Sokolov, K.; Aaron, J.; Hsu, B.; Nida, D.; Gillanwater, A.; Follen, M.; Macaulay, C.; Adler-Storthz, K.; Korgel, B.; Discour, M.; Pasqualini, R.; Arap, W.; Lam, W.; Richartz-Kortum, R. *Technol. Cancer Res. Treatment* **2003**, *2*(6), 491−504.
(9) Sokolov, K.; Follen, M.; Aaron, J.; Pavlova, I.; Malpica, A.; Lotan, R.; Richartz-Kortum, R. *Cancer Res.* **2003**, *63*, 1999−2004.
(10) Yelin, D.; Oron, D.; Thiberge, S.; Moses, E.; Silberberg, Y. *Opt. Express* **2003**, *11*, 1385−1391.
(11) Raub, C. B.; Orwin, E. J.; Haskell, R. *J. Biomech. Eng.* **2003**, *125*, 1−6.
(12) Yelin, D.; Oron, D.; Korkotian, E.; Segal, M.; Silberberg, Y. *Appl. Phys. B* **2002**, *74* (Suppl.), S97−S101.
(13) Yguerabide, J.; Yguerabide, E. E. *Anal. Biochem.* **1998**, *262*, 137−156.
(14) Yguerabide, J.; Yguerabide, E. E. *Anal. Biochem.* **1998**, *262*, 157−176.
(15) Hayat, M. A. *Principles and techniques of electron microscopy: biological applications*; Van Nostrand Reihold: New York, 1970.
(16) Nicholson, R. J.; Gee, J. M.; Harper, M. E. *Eur. J. Cancer* **2001**, *37* (Suppl. 4), S9−S15.

NL050074E